



# Crystal structures of two novel sulfonylurea herbicides in complex with *Arabidopsis thaliana* acetohydroxyacid synthase

Jian-Guo Wang<sup>1</sup>, Patrick K.-M. Lee<sup>2</sup>, Yu-Hui Dong<sup>3</sup>, Siew Siew Pang<sup>2,\*</sup>, Ronald G. Duggleby<sup>2,†</sup>, Zheng-Ming Li<sup>1</sup> and Luke W. Guddat<sup>2</sup>

<sup>1</sup> State Key Laboratory of Elemento-Organic Chemistry, National Pesticide Engineering Research Center, Nankai University, Tianjin, China

<sup>2</sup> School of Molecular and Microbial Sciences, The University of Queensland, Brisbane, Australia

<sup>3</sup> Beijing Synchrotron Radiation Facility, Institute of High Energy Physics, Beijing, China

## Keywords

acetohydroxyacid synthase; branched-chain amino acids; crystal structure; herbicide; sulfonylurea

## Correspondence

Z.-M. Li, State Key Laboratory of Elemento-Organic Chemistry, National Pesticide Engineering Research Center, Nankai University, Tianjin 300071, China

Fax: +86 22 2350 5948

Tel: +86 22 2350 3732

E-mail: nkzml@vip.163.com

L. W. Guddat, School of Molecular and Microbial Sciences, The University of Queensland, Brisbane, Qld 4072, Australia

Fax: +61 7 3365 4699

Tel: +61 7 3365 3549

E-mail: luke.guddat@uq.edu.au

## Present address

\*Department of Biochemistry, Monash University, Clayton, Australia

†RDBiotech, Little Mountain, Australia

## Database

Coordinates and structure factors have been deposited in the Protein Data Bank under the accession numbers 3E9Y and 3EA4

(Received 30 September 2008, revised 27 November 2008, accepted 18 December 2008)

doi:10.1111/j.1742-4658.2009.06863.x

## Abbreviations

AcThDP, acetyl thiamine diphosphate; AHAS, acetohydroxyacid synthase; AtAHAS, *Arabidopsis thaliana* acetohydroxyacid synthase; CSu, chlorsulfuron; HeThDP, hydroxyethyl thiamine diphosphate; IQ, imazaquin; MSE, monosulfuron ester; MSu, monosulfuron; ScAHAS, *Saccharomyces cerevisiae* acetohydroxyacid synthase; SM, sulfometuron methyl; ThDP, thiamine diphosphate.

The sulfonylurea herbicides are effective ultralow-dosage agrochemicals that are nontoxic to animals. This class of herbicides was first discovered by Levitt [1] via an extensive synthetic and screening program in the 1970s. Chlorsulfuron (CSu) (Fig. 1) was the first member of this family to be successfully developed from this study. This important achievement spawned the commercialization of dozens of sulfonylurea herbicides that have now benefited crop protection worldwide. The general features of the sulfonylureas (Fig. 1) are a central sulfonylurea bridge with an *o*-substituted aromatic ring attached to the sulfur atom, and a heterocyclic ring attached to the nitrogen atom. This

ring is substituted in both *meta*-positions, and can be either a pyrimidine ( $X = \text{CH}$ ) or a triazine ( $X = \text{N}$ ). Levitt [2] has summarized the structure–activity relationship of the sulfonylureas, and indicated that disubstitution at the *meta*-positions of the heterocyclic ring is absolutely required for this class of herbicide to have strong activity.

The target of the sulfonylurea herbicides was not known until it was discovered that sulfometuron methyl (SM) (Fig. 1) is a potent inhibitor of bacterial acetohydroxyacid synthase [3] (AHAS; EC 2.2.1.6), and that CSu inhibits plant AHAS [4]. AHAS is the first enzyme in the biosynthetic pathway of the branched-chain amino acids valine, leucine and isoleucine; a pathway that does not exist in animals [5]. The enzyme has three cofactors, thiamine diphosphate (ThDP),  $\text{Mg}^{2+}$  and FAD. The complete enzyme consists of two polypeptides: one of  $\sim 65$  kDa, which is the large or catalytic subunit, and a second regulatory subunit that varies between  $\sim 10$  and 50 kDa, depending on the organism [5,6].

The crystal structure of the complex between the catalytic subunit of *Saccharomyces cerevisiae* AHAS (*Sc*AHAS) and chlorsulfuron ethyl shows how the sulfonylureas bind to the herbicide-binding site [7]. The structures of five other sulfonylureas in complex with *Sc*AHAS have also been determined [8]. In 2006, the crystal structure of the catalytic subunit of *Arabidopsis thaliana* AHAS (*At*AHAS) was solved, in complex with five different sulfonylureas, and imazaquin (IQ), a member of the imidazolinone family of herbicides [9]. The active site of AHAS is located at the interface of two adjoining catalytic subunits at the base of a hydrophobic tunnel. Both the disubstituted sulfonylurea and imidazolinone herbicides bind at the entrance of this tunnel, preventing access of the substrate [7–9]. The conformation of the sulfonylurea herbicides when bound to either *Sc*AHAS or *At*AHAS is very similar, with a bend at the sulfonyl group that positions the two rings almost orthogonal to each other. The sulfonyl group and the adjacent aromatic ring are situated at the entrance to the tunnel leading to the active site, with the rest of the molecule inserting into the channel [7–9]. These structures have now explained the molecular basis of sulfonylurea herbicides and opened the way to the rational design of alternative inhibitors of AHAS.

Although most sulfonylurea herbicides obey Levitt's rule [2], that there should be substitution at both *meta*-positions of the heterocyclic ring, this requirement does not appear to be absolute. The crystal structures of AHAS in complex with these sulfonylureas [7–9] show there are numerous interactions between the herbicides

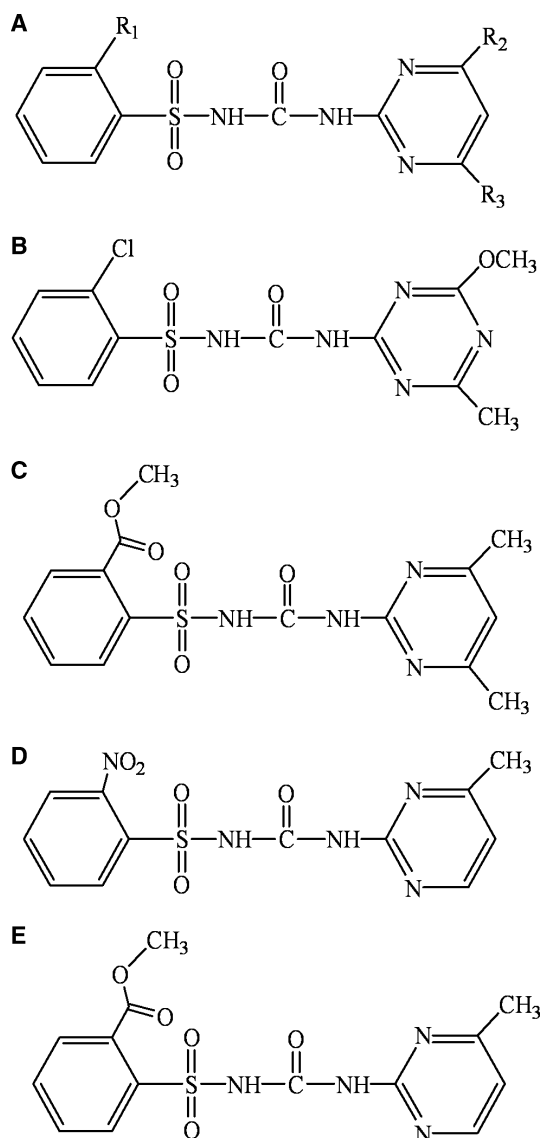


**Fig. 1.** Drawings of: (A) the general structure of the sulfonylureas; (B) CSu; (C) SM; (D) MSu; and (E) MSE.

and the protein, including contacts with the two aromatic rings and the sulfonylurea bridge. Thus, the requirement for both of the *meta*-substituents is not readily apparent. Indeed, Li *et al.* [10] have shown that some sulfonylurea compounds with only one substituent at the *meta*-position also exhibit significant herbicidal activity. Monosulfuron (MSu) and monosulfuron ester (MSE) are two examples (Fig. 1).

MSu and MSE have been developed as commercialized products after many years of basic research [11]. These herbicides can be used effectively to control weeds for a range of crops, including wheat, corn, rice, millet and peanuts, and can control both monocotyledonous and dicotyledonous weeds [10]. Moreover, MSu is a special herbicide for millet fields, where traditional disubstituted sulfonylurea herbicides are nonselective and there are no other effective herbicides currently available [12,13]. MSu has also been shown to be a specific herbicide for *Puccinella distans* Parl., a weed that is commonly observed in the alkaline soil of northern China, where it drastically affects the yield of wheat grown in these areas [13]. MSu and MSE have now been applied to 80 000 hectares of crops. Here, we report the crystal structures of MSu and MSE in complex with *At*AHAS at 3.0 and 2.8 Å resolution, respectively. Their smaller sizes as compared to the traditional sulfonylureas that obey Levitt's rules appear to give them a competitive edge in being less susceptible to resistance. Thus, understanding the mode of interaction for this class of inhibitors is important for the development of the next generation of herbicides based on sulfonylurea chemistry.

## Results

### *At*AHAS structure

The structures of the catalytic subunit of *At*AHAS in complex with MSu and MSE were determined to 3.0 and 2.8 Å resolution, respectively (Table 1). The overall folds of the polypeptides are similar to the previously determined structures of *At*AHAS in complex with the disubstituted sulfonylureas or IQ [7–9], with rmsd values for all C $\alpha$  atoms after superimposition in the range 0.17–0.23 Å. In the MSu and MSE complexes, the main chain and side chain atoms for all residues between 87 and 669 are visible in the electron density. Only the N-terminal amino acid, Thr86, and the C-terminal residue, Glu670, show no electron density. The asymmetric unit has one monomer of the catalytic subunit of *At*AHAS, FAD, a metal ion that we have assigned as Mg<sup>2+</sup>, as this was added to the crystallization media, an intermediate of ThDP, the

**Table 1.** Data collection and refinement statistics for *At*AHAS in complex with MSu and MSE.

	MSu	MSE
Crystal parameters		
Unit cell length (Å)	$a = b = 178.87$ , $c = 186.08$	$a = b = 178.47$ , $c = 184.95$
Unit cell angle (°)	$\alpha = \beta = 90.0$ , $\gamma = 120.0$	$\alpha = \beta = 90.0$ , $\gamma = 120.0$
Space group	$P6_422$	$P6_422$
Mosaicity (°)	0.534	0.612
Crystal dimensions (mm)	0.3 × 0.3 × 0.2	0.25 × 0.25 × 0.2
Diffraction data <sup>a</sup>		
Temperature (K)	100	100
Resolution range (Å)	89.44–3.00	58.42–2.80
Observations [ $I > 0\sigma(I)$ ]	186 539	249 940
Unique reflections [ $I > 0\sigma(I)$ ]	28 796	42 923
Completeness (%)	80.5 (82.5)	98.7 (96.4)
$R_{\text{sym}}^b$	0.072 (0.228)	0.075 (0.315)
$\langle I \rangle / \langle \sigma(I) \rangle$	22.5 (4.5)	20.1 (2.4)
Monomers per asymmetric/unit	1	1
Solvent content (Å <sup>3</sup> /Da)	81.23	80.78
Matthews coefficient (Å <sup>3</sup> /Da)	6.61	6.45
Refinement		
Resolution limits (Å)	89.44–3.00	58.42–2.80
$R_{\text{factor}}$	0.1922	0.1990
$R_{\text{free}}$	0.2235	0.2134
rmsd bond lengths (Å)	0.006	0.007
rmsd bond angles (°)	1.106	1.153
Ramachandran plot (%)		
Most favored	90.4	91.6
Additionally allowed	9.4	7.9
Generously allowed	0.2	0.4
Disallowed	0.0	0.0

<sup>a</sup> Values in parentheses are for the outer resolution shell: 3.11 to 3.00 Å for MSu and 2.90 to 2.80 Å for MSE. <sup>b</sup>  $R_{\text{sym}} = \sum |I - \langle I \rangle| / \sum \langle I \rangle$ , where  $I$  is the intensity of an individual measurement of each reflection and  $\langle I \rangle$  is the mean intensity of that reflection.

herbicide inhibitor, and a 2-(*N*-cyclohexylamino)ethanesulfonic acid molecule, also from the crystallization solution. The tetramer is defined by four molecules related by crystallographic symmetry. In total, 65 and 108 water molecules were modeled into the electron density for the MSu and MSE complexes, respectively. The electron density map shows that Cys340 is modified to the sulfinic acid derivative of cysteine, a rare occurrence in protein structures, usually associated with proteins that function in oxidation and reduction [14]. However, its presence here appears to be solely to fill space in the core of the protein, with the terminal oxygen atoms of this side chain forming hydrogen bonds with a buried water molecule and the backbone nitrogen of Tyr498. Cys340 is at least 11 Å

from the closest FAD and 18 Å from the closest ThDP, and is not situated at a subunit interface. Thus, this residue is unlikely to be directly involved in catalysis or in stabilizing the quaternary structure of the catalytic subunit of *At*AHAS.

As reported in the structures of *At*AHAS in complex with the disubstituted sulfonylureas and with IQ, a prolyl *cis*-peptide bond is observed between Leu648 and Pro649 in the MSu and MSE complexes. We have previously hypothesized that this residue acts as a rotation point that commences the ordering the C-terminal tail [9]. No other post-translational modifications or unusual polypeptide geometries are present in either structure (Table 1).

In both the MSu and MSE complex structures, the isoalloxazine ring of the FAD adopts a bent conformation. In all of the *At*AHAS structures determined to date, the isoalloxazine ring of FAD adopts a similar conformation [6]. Figure 2 shows a stereo diagram of the location of MSu, FAD and a ThDP intermediate within *At*AHAS.

### ThDP

In all of the previously determined structures of *At*AHAS in complex with the disubstituted sulfonylureas [9], ThDP cannot be accommodated into the electron density, which is severely diminished at the C2 carbon atom and through portions of the regions where the thiazolium and pyrimidine rings would be located. In contrast, in the structure of *At*AHAS where the imidazolinone IQ is bound, the electron density is complete for ThDP. It was therefore somewhat unexpected to observe that in the structures of MSu and MSE in complex with *At*AHAS, the ThDP had complete electron density, as well as additional electron density attached to the C2 atom (Fig. 3). The shape of this density was consistent with that of a planar group of three nonhydrogen atoms attached to the C2 atom. On the basis of this, two intermediates are possible, either hydroxyethyl-ThDP (HeThDP) or acetyl-ThDP (AcT-

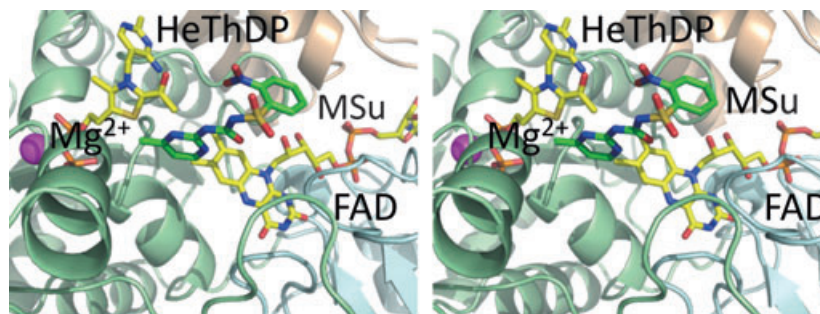
hDP). It has, however, been shown that the HeThDP can be dramatically stabilized within the environment of an AHAS from *Escherichia coli* [15]. Thus, we favor the interpretation that HeThDP is observed.

In both the MSu and MSE complexes, the pyrimidine ring of ThDP is held by hydrophobic contacts to Tyr118', Pro170', and Met513, and by hydrogen bonds to Gly120', Glu144', and Gln207' [where the prime (') symbol represents residues from an adjoining subunit], and the thiazolium ring is held by hydrophobic contacts with Gly120', Met513, Leu568, Met570, and Val571. The diphosphate tail of ThDP is hydrogen bonded to Gln487, His488, Asp538, Gly539, Ser540, His567, and Gly569. The metal ion is coordinated to two of the diphosphate oxygen atoms, to the side chains of Asp538 and Asn565, and to the backbone oxygen atom of His567.

The overall structure of the HeThDP intermediate has a V-conformation as defined by the bond angle between the C5' and C7' atoms of the pyrimidine ring and the N3 atom of the thiazolium ring (Fig. 3). This bond angle is 104° and 107° when it is in complex with MSu and MSE, and 113° when IQ is bound to *At*AHAS.  $\Phi_T$  and  $\Phi_P$ , the dihedral angles between C4', C5', C7' and N3, and C5', C7', N3 and C2, respectively, provide an additional measurement of the relative orientation of the two rings. These values are -56° and 109° in the MSu complex, -53° and 103° in the MSE complex, and -61° and 104° in the IQ complex. Overall, these differences represent a small perturbation in the conformation of the rings when the HeThDP is present. Superimposition of the structures of the MSu complex (with HeThDP) and the IQ complex (with ThDP) shows that C2 moves towards Gln207' by 0.7 Å (Fig. 3).

The assignment of the positions for the hydroxyl oxygen and the terminal carbon atom of the HeThDP intermediate cannot be determined unambiguously on the basis of the electron density alone, as these atoms are indistinguishable at the resolution of the structures that have been determined. However, one of the atoms

**Fig. 2.** Stereo diagram of the active site of a single subunit of the MSu–*At*AHAS complex. The individual domains, 87–281, 282–452 and 464–640, are colored brown, blue and green, respectively. ThDP, FAD and MSu are shown as stick models, and Mg<sup>2+</sup> as a magenta sphere.





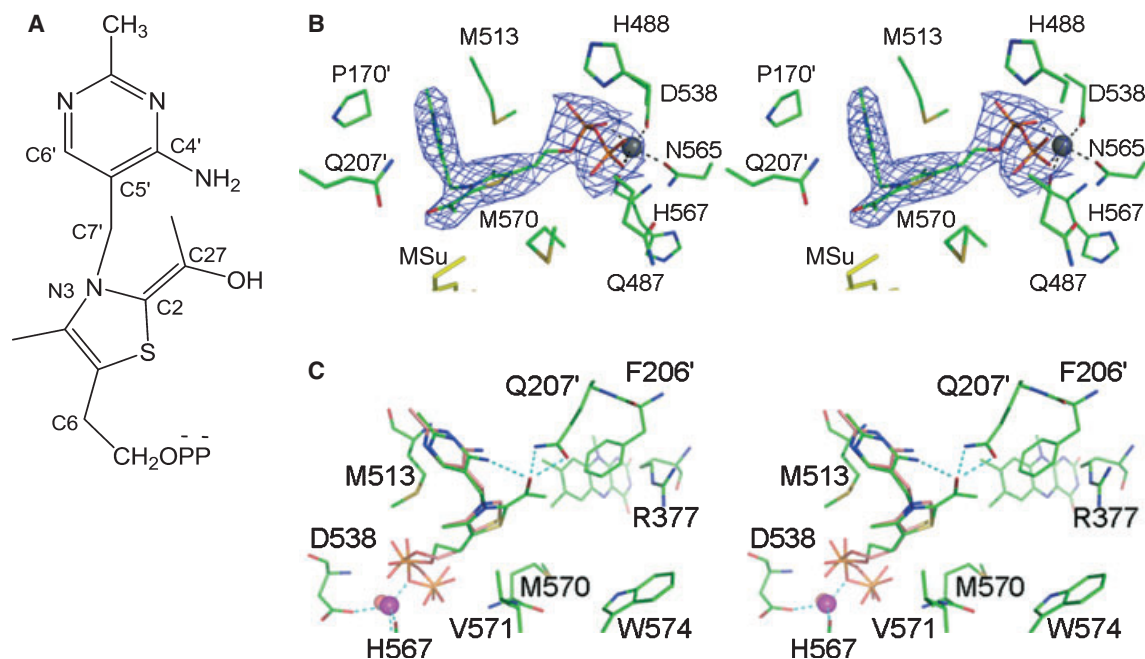


**Fig. 3.** HeThDP. (A) The chemical structure for HeThDP with some atoms labeled. (B) Stereo diagram of the electron density for HeThDP and the active site of AtAHAS. Neighboring active site amino acid side chains, a portion of MSu (yellow) and  $Mg^{2+}$  as a gray sphere are also shown. The  $F_o - F_c$  electron density (contoured  $3.5\sigma$ ) for HeThDP is overlaid in blue mesh. (C) Stereo diagram of HeThDP in the AtAHAS complex with MSE, with ThDP from the IQ-AtAHAS complex overlaid in brown.

is close enough ( $\sim 2.6\text{--}2.8 \text{ \AA}$ ) to form hydrogen bonds to the side chain oxygen and nitrogen atoms of Gln207' and to a nitrogen of the pyrimidine ring. We therefore assign this as the hydroxyl group. The formation of these hydrogen bonds appears to be the reason why the C2 atom has moved and why there are small differences in bond and dihedral angles when the structures of HeThDP and ThDP are compared. In comparing the structures of AtAHAS when HeThDP, ThDP and the degraded ThDP are present, the side chain of Gln207 adopts different conformations, but its position is stabilized by the formation of these hydrogen bonds in the presence of HeThDP. This stabilization is further reflected in a reduction of the average  $B$ -value for the side chain atoms of this residue by  $\sim 10 \text{ \AA}^2$  (relative to the backbone atoms in this location).

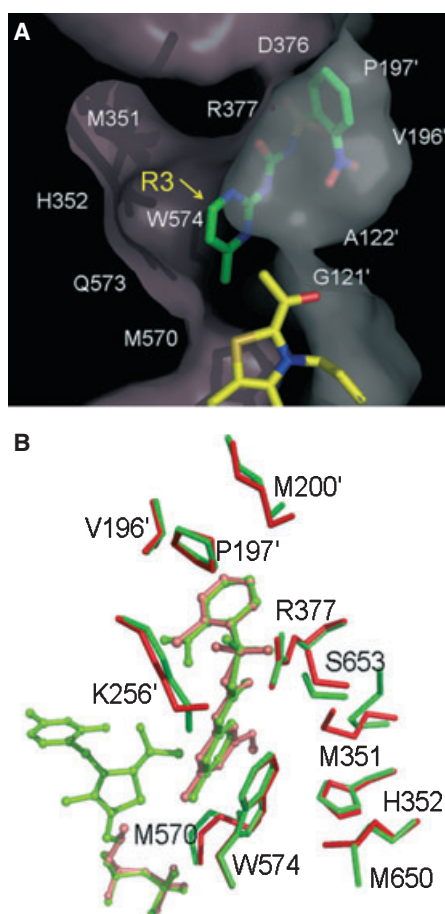
In a survey of 24 AHAS sequences, Gln207 is completely conserved [16], emphasizing its importance in the activity of the enzyme, where its role has been suggested to be in proton transfer to the second substrate during catalysis [17]. In the conformation observed in these structures, and in the absence of the inhibitors, there is sufficient space to allow addition of the second substrate, either pyruvate or 2-ketobutyrate.

Figure 3 shows that there are differences in position of the ethylene carbon atoms and the phosphate

oxygen atoms of ThDP when this structure is compared to that of the IQ-bound structure. However, similar variations are also observed in the fragmented versions of ThDP, suggesting that these variations are unrelated to the presence of the bound intermediate. Furthermore, the C6 atoms of ThDP are less than  $0.4 \text{ \AA}$  apart after the superimposition of the MSE and IQ complexes, indicating that there are no transmitted conformation changes in the diphosphate tail due to the presence of the intermediate.

### MSu and MSE inhibitors

The  $K_i$  values for AtAHAS for MSu and MSE are 245 and 363 nM. For the most closely analogous disubstituted sulfonyleureas for which structures have been determined, CSu and SM, the  $K_i$  values are 14.4 and 39.5 nM, respectively. Both MSu and MSE occupy a similar location (Fig. 4) as for the disubstituted sulfonyleureas when bound to AtAHAS, with both inhibitors adopting an L-shaped structure such that there is a bend at the sulfonyl group making the two rings orthogonal to each other. The methyl group at R<sub>2</sub> (Figs 1, 2 and 4) on the heterocyclic ring is inserted deepest into the active site and is in a location that is bordered by Trp574, Met570, and HeThDP. In both structures, there is no electron density at the



**Fig. 4.** MSu in the herbicide-binding site. (A) The *AtAHAS* polypeptide surface is shown as purple and white Connolly surfaces for the different subunits. The region where the  $R_3$  substituent in the disubstituted sulfonylureas is located is unoccupied. This site is identified by the yellow label and arrow. MSu and HeThDP are drawn as stick models, with green carbon atoms for MSu and yellow carbon atoms for HeThDP. (B) Structures of *AtAHAS* in complex with MSu superimposed on the structure with CSu. Residues within 4 Å of MSu or CSu are shown as green or red sticks respectively. MSu and CSu are depicted as light green or pink ball and stick models. HeThDP from the MSu complex is depicted as a light green ball and stick model, and the ethylene diphosphate from the CSu structure is shown as a pink ball and stick model.

alternative position for the methyl group on the heterocyclic ring; there is thus a clear preference for the methylpyrimidine group to bind in this orientation.

The  $K_i$  values for MSu and MSE are ninefold to 17-fold higher than for their disubstituted sulfonylurea counterparts [12]. Overall, there are few differences in the mode of binding of monosubstituted and disubstituted sulfonylurea herbicides to the enzyme. A comparison of the modes of binding of MSu and CSu to *AtAHAS* is shown in Fig. 4. CSu was chosen for comparison because its structure is most similar to that

of MSu, with the only differences being that CSu has a methoxy group at  $R_3$  and MSu has a hydrogen atom in this position, whereas at  $R_1$ , MSu has an  $\text{NO}_2$  and CSu has a chlorine atom (Fig. 1). The most obvious differences are a slight change in orientation of the side chain nitrogen atom of Lys256, and the side chain of Met351 adopting a different conformation in the MSu complex. The side chains of both of these amino acids are attracted to the methoxy group of CSu by several van der Waals interactions (the groups are  $\sim 3.7$  Å apart). In the MSu complex, where this methoxy group is absent, these side chains are rotated away, with Met351 forming hydrophobic contacts with Gly380, and Met570 forming contacts with Met490.

For MSE, the closest comparison with a disubstituted sulfonylurea is with SM, where the only difference is that SM contains an additional methyl group at  $R_3$  (Fig. 1). In the resulting superimposition, no significant changes in the conformations of the surrounding amino acid side chains were observed. Thus, it again appears that the addition of the methyl group is mostly responsible for the ninefold difference in  $K_i$  values for these two inhibitors. Thus, overall, the major difference seen when comparing the monosubstituted and disubstituted sulfonylureas is that the space occupied by the second substituent of the heterocyclic ring is not filled in either the MSu or MSE complex structures, resulting in a gap between the herbicide and the enzyme at this position. This would appear to be the major steric reason for the reduction in binding affinity between the enzyme and this class of inhibitor. Another factor for consideration is the difference in electrostatic properties between the disubstituted and monosubstituted heterocycles. The  $\pi$  stacking interaction between the heterocyclic ring and Trp574 is of critical importance to the binding of the sulfonylureas to AHAS. The disubstituted aromatic ring is more electron-rich, owing to inductive electron donation of the two methyl groups, and therefore would have a stronger attraction for Trp574 than a monosubstituted ring.

## Discussion

The use of herbicides in farming is a relatively recent phenomenon, with their widespread use resulting in a significant increase in global crop production. However, with their constant use, it is inevitable that resistant weed strains will begin to emerge. The sulfonylureas and imidazolinones that target AHAS are particularly susceptible to resistance, because their binding sites do not correspond to the active site but to a tunnel that allows substrate access to the active

site [9]. Thus, mutations that interfere with herbicide binding can still yield enzymes that are catalytically active. One approach to the development of improved herbicides that target AHAS and are less susceptible to resistance is to design inhibitors that bind directly to the active site. An alternative approach to reducing an organism's ability to construct effective resistance sites is to simplify existing herbicides, thereby providing fewer options for mutations that affect binding. MSu and MSE are smaller versions of the classic sulfonylureas, and bind to AHAS with fewer contacts. As a result of the removal of one of the substituents from the heterocyclic ring, MSu and MSE have greater flexibility of fit within the herbicide-binding site, and therefore their binding can be less affected by a single mutation than that of the disubstituted sulfonylureas. The most commonly observed mutation in the field is W574L. The reason that this mutation is so effective is that the  $\pi$  stacking between this residue in the enzyme and the heterocyclic ring of the inhibitor is removed. Furthermore, the shape of the herbicide-binding site is altered, preventing the herbicide from optimally binding to AHAS. This structural change appears to be the molecular basis for the fact that, under specialized conditions such as those that prevail in the alkaline soil regions of northern China, monosubstituted sulfonylureas are now more effective herbicides than their disubstituted counterparts.

The mode of binding of MSE in the herbicide-binding site does not differ significantly from that of SM. The residues that are critical in holding the inhibitor in place are similar. The difference in  $K_i$  appears to be mainly due to the extra methyl group at  $R_3$ , which fills space in the binding site, allowing a more complementary interaction with the enzyme.

We suggest that HeThDP is observed in the structures of *At*AHAS in complex with MSu or MSE. This finding is surprising in two ways. First, the intermediates can only form upon the addition of substrates to the enzyme, and in these experiments no pyruvate or other substrate was added to the enzyme. Second, ThDP is intrinsically unstable when bound to AHAS [18] or other ThDP-dependent enzymes [19,20]. There are two possible reasons for the presence of the intermediate. Either the intermediate or pyruvate is present throughout the purification of the enzyme, or pyruvate is present as an impurity in the crystallization media. We have analyzed by MS all of the components of the crystallization media individually and combined, and found no evidence for the presence of pyruvate in any of these solutions. Thus, the source of the intermediate cannot be determined. Nonetheless, the structure provides a good model for the bound intermediate,

providing a solid basis for understanding the polar interactions between the enzyme and the intermediate. In the previous structures of AHAS in complex with sulfonylureas [8,9], it is hypothesized that sulfonylurea binding and the subsequent closure of the active site led to the formation of the carbanion of ThDP, which in turn led to the degradation of ThDP. However, upon binding of MSu and MSE, this clearly does not occur. The monosubstituted sulfonylureas generally exhibit a looser fitting to the enzyme than their disubstituted counterparts, and this difference therefore appears to lead to the accumulation of HeThDP. In this complex, the HeThDP intermediate is stabilized within the active site, where it forms a hydrogen bond to Gln207, which is postulated to be involved in proton transfer during catalysis. In this arrangement, ThDP appears to be less susceptible to breakdown, particularly when subjected to X-rays, which may be a cause of the breakdown [21] observed in the disubstituted sulfonylurea complexes.

This article describes the binding of two new members of the sulfonylurea family of herbicides, MSu and MSE. These structures have enabled us to understand the relative importance of the groups at  $R_2$  and  $R_3$  (Fig. 1). These structures represent the first experimental visualization of the AHAS reaction mechanism at the point of HeThDP formation, and provide new data for use in further rational structure-based inhibitor design.

## Experimental procedures

### Synthesis of sulfonylureas

MSu and MSE were synthesized using procedures detailed by Li *et al.* [22,23].

### AHAS expression and purification

The DNA sequence encoding the mature catalytic subunit of *At*AHAS (after removal of the chloroplast transit peptide) was subcloned into the pET30a(+) vector to introduce a C-terminal hexahistidine tag. This plasmid was used to transform *E. coli* strain BL21(DE3) cells. Expression and purification was as described previously [24], except that the enzyme was concentrated to 27 mg·mL<sup>-1</sup> prior to being stored in small aliquots at -70 °C for crystallization trials.

### Crystallization and structure determination

Crystallization of the complexes with MSu and MSE was as described previously for disubstituted sulfonylurea herbicides [24]. Briefly, the crystals were prepared by hanging

drop vapor diffusion using a well solution consisting of 0.1 M 2-(*N*-cyclohexylamino)-ethanesulfonic acid, 0.2 M Li<sub>2</sub>SO<sub>4</sub> and 1.0 M potassium sodium tartrate (pH 9.4). The drop consisted of well solution mixed with an equivalent volume of protein solution consisting of 1 mM ThDP, 1 mM FAD, 1 mM MgCl<sub>2</sub>, 5 mM dithiothreitol, and 1 mM MSu or MSE. For cryoprotection, crystals were transferred to a well solution that also contained 30% (v/v) ethylene glycol. Both datasets were collected on Beam-Line 14C at the Advanced Photon Source in the Argonne National Laboratory (Chicago, IL, USA). The crystal-to-detector distance was 260 mm, and 300 images of 15 s exposure with an oscillation range of 0.2° each were obtained for both datasets. The data were indexed, integrated and scaled using the programs DENZO and SCALEPACK [25].

Restrainted refinement of the structures with translation, libration and screw-rotation displacements for the three domains of each subunit was initially undertaken using the polypeptide coordinates of the catalytic subunit of AtAHAS in complex with chlorimuron ethyl, ThDP, Mg<sup>2+</sup> and FAD (Protein Data Bank code: 1YBH), using REFMAC5 [26]. Model building into the electron density for the polypeptide, cofactors, solvent and inhibitor molecules was performed with the program COOT [27]. All of the figures were prepared with CHEMDRAW [28] or PYMOL (DeLano Scientific, LLC) [29].

## Acknowledgements

Preliminary X-ray data were obtained using facilities provided by the University of Queensland Macromolecular X-ray Crystallography (UQROXCS) facility. The use of the BioCARS sector was supported by the Australian Synchrotron Research Program, which is funded by the Commonwealth of Australia under the Major National Research Facilities Program. Use of the Advanced Photon Source was supported by the US Department of Energy, Basic Energy Sciences, Office of Energy Research, under Contract No. W-31-109-Eng-38. We thank K. Brister and H. Tong for help with data collection at the Advanced Photon Source. This work was supported by grant DP0450275 from the Australian Research Council, National Basic Research Program of China (Grant No. 2003CB114406) and National Natural Science Foundation Project of China (Grant No. 20432010 and 20602021).

## References

- Levitt G (1978) Herbicidal sulfonamides. Patent no. 4127405, US patent office.
- Levitt G (1991) Discovery of the sulfonyleurea herbicides. In *Synthesis and Chemistry of Agrochemicals II*. ACS Symposium Series 443 (Baker DR, Fenyves JG & Moberg WK, eds), pp. 16–31. American Chemical Society, Washington, DC.
- LaRossa RA & Schloss JV (1984) The sulfonyleurea herbicide sulfometuron methyl is an extremely potent and selective inhibitor of acetolactate synthase in *Salmonella typhimurium*. *J Biol Chem* **259**, 8753–8757.
- Ray TB (1984) Site of action of chlorsulfuron: inhibition of valine and isoleucine biosynthesis of plants. *Plant Physiol* **75**, 827–831.
- Duggleby RG & Pang SS (2000) Acetohydroxyacid synthase. *J Biochem Mol Biol* **33**, 1–36.
- Duggleby RG, McCourt JA & Guddat LW (2008) Structure and mechanism of inhibition of plant acetohydroxyacid synthase. *Plant Physiol Biochem* **46**, 309–324.
- Pang SS, Guddat LW & Duggleby RG (2003) Molecular basis of sulfonyleurea herbicide inhibition of acetohydroxyacid synthase. *J Biol Chem* **278**, 7639–7644.
- McCourt JA, Pang SS, Guddat LW & Duggleby RG (2005) Elucidating the specificity of binding of sulfonyleurea herbicides to acetohydroxyacid synthase. *Biochemistry* **44**, 2330–2338.
- McCourt JA, Pang SS, King-Scott J, Guddat LW & Duggleby RG (2006) Herbicide-binding sites revealed in the structure of plant acetohydroxyacid synthase. *Proc Natl Acad Sci USA* **103**, 569–573.
- Li Z-M, Jia G-F, Wang L-X, Fan C-W & Yang Z (1998) Novel sulfonyleurea herbicides. Chinese Invention Patent ZL 94118793.4.
- Li Z-M & Lai CM (2001) Research on the structure/activity relationship on herbicidal sulfonyleureas. *Chin J Org Chem* **21**, 810–815.
- Wang L-X, Li Z-M, Jia G-F, Chen J-P & Wang S-H (2003) The application of monosulfuron in millet fields. Chinese Invention Patent ZL 98100257.9.
- Wang JG, Li ZM, Ma N, Wang BL, Jiang L, Pang SS, Lee YT, Guddat LW & Duggleby RG (2005) Structure–activity relationships for a new family of sulfonyleurea herbicides. *J Comput Aided Mol Des* **19**, 801–820.
- Jacob C, Holme AL & Fry FH (2004) The sulfenic acid switch in proteins. *Org Biomol Chem* **2**, 1953–1956.
- Tittmann K, Schroder K, Golbik R, McCourt J, Kaplun A, Duggleby RG, Barak Z, Chipman DM & Hubner G (2004) Electron transfer in acetohydroxy acid synthase as a side reaction of catalysis. Implications for the reactivity and partitioning of the carbanion/enamine form of ( $\alpha$ -hydroxyethyl) thiamin diphosphate in a ‘nonredox’ flavoenzyme. *Biochemistry* **43**, 8652–8661.
- McCourt JA & Duggleby RG (2006) Acetohydroxyacid synthase and its role in the biosynthetic pathway for branched-chain amino acids. *Amino Acids* **31**, 173–210.
- Engel S, Vyazmensky M, Vinogradov M, Berkovich D, Bar-Ilan A, Qimron U, Rosiansky Y, Barak Z &



- Chipman DM (2004) Role of a conserved arginine in the mechanism of acetohydroxyacid synthase: catalysis of condensation with a specific ketoacid substrate. *J Biol Chem* **279**, 24803–24812.
- 18 McCourt JA, Nixon PF Duggleby RG (2006) Thiamin nutrition and catalysis-induced instability of thiamin diphosphate. *Br J Nutr* **96**, 636–638.
- 19 Abell LM & Schloss JV (1991) Oxygenase side reactions of acetolactate synthase and other carbanion-forming enzymes. *Biochemistry* **30**, 7883–7887.
- 20 Dobritzsch D, König S, Schneider G & Lu G (1998) High resolution crystal structure of pyruvate decarboxylase from *Zymomonas mobilis*. Implications for substrate activation in pyruvate decarboxylases. *J Biol Chem* **273**, 20196–20204.
- 21 Burmeister WP (2000) Structural changes in a cryo-cooled protein crystal owing to radiation damage. *Acta Crystallogr D* **56**, 328–334.
- 22 Wang J-G, Ma N, Wang B-L, Wang S-H, Song H-B & Li Z-M (2006) Synthesis, crystal structure and biological activity of *N*-(4-methylpyrimidin-2-yl)-*N'*-2-(nitrophenylsulfonyl)urea and its docking with yeast AHAS. *Chin J Org Chem* **26**, 648–652.
- 23 Wang B-L, Ma N, Wang J-G, Ma Y, Li Z-M & Leng X-B (2004) Synthesis and dimeric crystal structure of sulfonyleurea compound *N*-[2-(4-methyl)pyrimidinyl]-*N'*-2-methoxycarbonyl-benzene sulfonyleurea. *Chin J Struct Chem* **23**, 783–787.
- 24 Pang SS, Guddat LW & Duggleby RG (2004) Crystallization of *Arabidopsis thaliana* acetohydroxyacid synthase in complex with the sulfonyleurea herbicide chlorimuron ethyl. *Acta Crystallogr D* **60**, 153–155.
- 25 Otwinowski Z & Minor W (1997) Processing of x-ray diffraction data collected in oscillation mode. *Methods Enzymol* **276**, 307–326.
- 26 Potterton E, Briggs P, Turkenburg M & Dodson E (2003) A graphical interface to the CCP4 program suite. *Acta Crystallogr D* **59**, 1131–1137.
- 27 Emsley P & Cowtan K (2004) Coot: model-building tools for molecular graphics. *Acta Crystallogr D* **60**, 2126–2132.
- 28 CambridgeSoft Corp (2005) *Chemdraw*. CambridgeSoft Corp., Cambridge, MA.
- 29 DeLano WL (2002) *The PyMOL Molecular Graphics System*. DeLano Scientific, San Carlos, CA.